Appl Phys A (2011) 103: 915–919
DOI 10.1007/s00339-010-6237-4

Applied Physics A
Materials Science & Processing

Application of the McCutchen theorem to image-forming metamaterial slabs

Carlos J. Zapata-Rodríguez · Juan J. Miret

Received: 30 March 2010 / Accepted: 3 December 2010 / Published online: 7 January 2011

Abstract A nonsingular, polarization-dependent, 3D impulse response is derived to determine unambiguously the amplitude distribution in the image volume of a negative-refractive-index layered lens. The generalized amplitude transfer function is introduced to gain a deep insight into the resolution power of the optical element. In the near-field regime, fine details containing some depth information may be transmitted through the lens. Metamaterials with moderate absorption are appropriate for subwavelength resolution keeping a limited degree of depth discrimination.

1 Introduction

The possibility of recovering subwavelength details of an object is a subject of growing interest leading to a profusion of superresolving image-forming techniques. In 2000 Pendry [1] showed that a thin slab of a medium with negative refractive index (NRI) is capable of generating an exact replica of a plane object, thus being coined as a perfect lens. For the homogeneous part of the field, a phase reversal is accomplished within the NRI medium that compensates the phase gathered by the wave when traveling away from the source. On the other hand, the evanescent components of the wavefield carrying those subwavelength features are amplified in the metamaterial layer in order to regain their amplitudes at the image plane. To do it, coupled surface plasmons are excited at the input and output interfaces of the NRI-material slab. Unfortunately, absorption inherent in NRI media restrains a perfect lens from ideal reconstruction of the object.

To derive the resolution limit of the system, the amplitude transfer function (ATF) has been preferably examined since it provides straight the cutoff frequency beyond which one cannot find any spectral component in the reconstructed image. Thus separating the s-polarized and p-polarized components of the field, the image-forming metamaterial layer behaves as a linear and shift-invariant system having a scalar transfer function [2]. As a consequence, the response of the imaging slab for each polarization may be developed by means of the point spread function (PSF), resulting from the Fourier transform of the corresponding ATF.

In a complementary analysis the Rayleigh criterion of resolution may be adopted, for which two point sources are just resolved when the first diffraction minimum of the image of one object point coincides with the maximum of the adjacent source. Thus the PSF may be referred to a resolution gauge for our optical element since the full width of its central peak may be used to measure the limit of resolution. Moreover, in optical microscopy we generally have point sources placed at different distances from the layered lens leading to different limits of resolution along a direction either parallel or perpendicular to the surfaces. Specifically the transverse resolution has been studied in detail but little is said about axial resolution of these metamaterial image formers [3].

In this paper we introduce the generalized ATF, identifying a closed-surface sheet for the far field and a hyperboloid sheet for the evanescent-wave component. From the geometry of the generalized ATF we interpret the PSF pattern in the image volume. Moreover, this allows us to provide some

C.J. Zapata-Rodríguez (✉)
Departamento de Óptica, Universidad de Valencia,
Dr. Moliner 50, 46100 Burjassot, Spain
e-mail: carlos.zapata@uv.es

J.J. Miret
Departamento de Óptica, Universidad de Alicante, P.O. Box 99,
Alicante, Spain
e-mail: jjmiret@ua.es

relevant aspects on the depth-discrimination capabilities of the perfect lens.

2 Image formation with NRI slabs

Let us consider a thin metamaterial slab with its front face (input plane) at $z = 0$ and the output plane at $z = d$ thus d denoting the layer width. This optical element depicted in Fig. 1(a) will generate an image in the semi-space $z \geq d$ from a given plane object laying on $z = -z_0$ ($z_0 \geq 0$). For simplicity we assume that both object and image media are the vacuum. To have a high-fidelity reproduction at the image plane, the negative index of refraction n_2 of the metamaterial should coincide in magnitude with that of the object (and image) medium ($n_1 = 1$). Material losses prevent from this ideal situation and we therefore assume a realistic, simple model, in which permittivity and permeability are of the form $\epsilon_2 = \mu_2 = -1 + i\delta$. Under these circumstances perfect imaging cannot be achieved since $n_2 = -1 + i\delta$. However a good replica may be found at the plane $z = 2d - z_0$ if $\delta \ll 1$. Moreover, the condition $0 \leq z_0 \leq d$ leads to real images in $d \leq z \leq 2d$.

In order to determine the wave fields in the image plane, it is customary to separate the s-polarized waves ($E_z = 0$) from the p-polarized waves ($H_z = 0$) constituting the electromagnetic field emitted by the source. Nieto-Vesperinas [2] showed that the *perfect* lens is a linear and 3D shift-invariant (3D LSI) system. For s-polarized waves, the transverse electric (TE) field emerging from the NRI slab satisfies

$$\vec{E}_{\text{out}}(\vec{R}, z) = \iint \vec{E}_{\text{in}}(\vec{R}_0, -z_0) h_3 \times (\vec{R} - \vec{R}_0, z - 2d + z_0)\, d^2\vec{R}_0, \tag{1}$$

where $\vec{E}_{\text{in}}(\vec{R}_0, -z_0)$ is the TE wave field at the object plane traveling in the direction to the input plane. We recognize the 3D function

$$h_3(\vec{R}, z) = (2\pi)^{-2} \iint T(\vec{k}_\perp) \times \exp\left(i\vec{k}_\perp \vec{R}\right) \exp(i\beta_1 z)\, d^2\vec{k}_\perp, \tag{2}$$

as the PSF of the optical system. In (2), the layer transmittance

$$T(\vec{k}_\perp) = \frac{t_{12}t_{21}\exp[i(\beta_1 + \beta_2)d]}{1 - r_{21}^2 \exp(2i\beta_2 d)}, \tag{3}$$

follows the Airy formula [5] except for a linear phase factor. If $k_0 = 2\pi/\lambda_0$ denotes the wavenumber in vacuum, the propagation constant reads

$$\beta_j = \sigma_j \sqrt{k_0^2 \epsilon_j \mu_j - \vec{k}_\perp \cdot \vec{k}_\perp}, \quad \text{for } j = \{1, 2\}. \tag{4}$$

Note that $\sigma_1 = 1$ for the vacuum and $\sigma_2 = -1$ for the NRI material. Also

$$r_{jk} = \frac{\mu_k \beta_j - \mu_j \beta_k}{\mu_k \beta_j + \mu_j \beta_k} \tag{5}$$

is the reflection coefficient for s-polarized waves at a single interface, and $t_{jk} = r_{jk} + 1$.

For p-polarized waves it is convenient to derive first the transverse magnetic (TM) field $\vec{H}_{\text{out}}$ $(\vec{R}, z \geq d)$ from that TM field at the object plane $\vec{H}_{\text{in}}$ $(\vec{R}_0, -z_0)$. This yields a convolution similar to (1), where its PSF may be written again into the plane-wave representation (2) by means of the layer transmittance (3). It is well known that the substitutions $\epsilon_j \leftrightarrow \mu_j$ switches the Airy formula for TM waves and TE waves, respectively [5]. In our case, however, both material parameters are set equal providing an unique PSF.

Disregarding material losses ($\delta = 0$) we have $T = 1$ yielding $h_3(\vec{R}, 0) = \delta_2(\vec{R})$. In this limiting case [1], the presence of the 2D Dirac delta function δ_2 leads to a perfect image

$$\vec{E}_{\text{out}}(\vec{R}, 2d - z_0) = \vec{E}_{\text{in}}(\vec{R}_0, -z_0). \tag{6}$$

However $h_3(\vec{R}, z)$ would exhibit a singular behavior in $z < 0$ [2]. Thus absorption δ acts as a regularizing parameter that provides a Wiener-like filter T.

The amplitude of the 3D PSF $|h_3|$ is depicted in Fig. 1(b) for NRI slabs of different widths d. Since T is radially symmetric, the PSF varies upon the axial coordinate z and the modulus of the transverse vector, R. In the numerical simulation we set a wavelength $\lambda_0 = 600$ nm in vacuum, and losses $\delta = 0.1$ for the metamaterial. Shifting the image plane at $z = 0$, the exit surface of the layered lens would be found at $z = z_0 - d$. Bearing in mind that $z_0 \geq 0$, the meaningful part of the PSF lies within the range $z \geq -d$ as considered in the graphical representation. The 3D amplitude distribution of the PSF for a subwavelength width d shows a distinct behavior in comparison with those impulse responses for $d \gg \lambda_0$. For instance, the FWHM of the PSF at the image plane $\Delta_\perp = 73.5$ nm is clearly subwavelength at $d = 60$ nm; in fact $\Delta_\perp$ would vanish if d were identically zero. Moreover, the amplitude reaches a maximum value at the center point $R = 0$ on the output plane. On the contrary, $\Delta_\perp = 552$ nm comes near the wavelength at $d = 1.8$ μm. Here the maximum amplitude is found approaching the image plane far from the output plane, existing a small longitudinal shift of 104 nm. Furthermore one may determine a FWHM along the z-axis, and in our case we found $\Delta_z = 1.70$ μm.

3 The generalized ATF

A convenient interpretation of these results is derived by writing explicitly the far-field term and the evanescent-wave

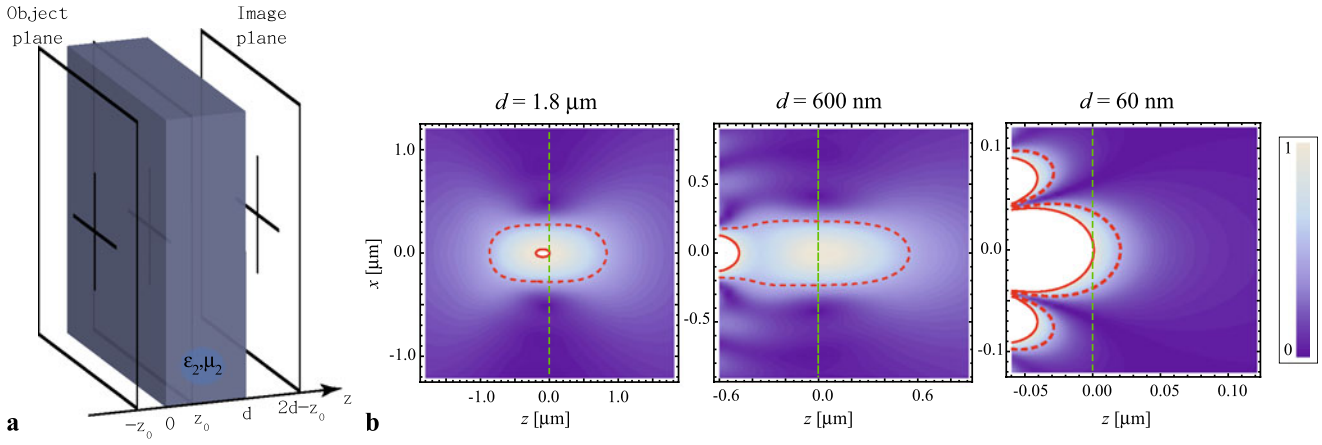

Fig. 1 **(a)** Schematic geometry of the planar-layer-based perfect lens. **(b)** Absolute value of the PSF $|h_3|$ in $z \geq -d$ at $\lambda_0 = 600$ nm for absorbing slabs of $\delta = 0.1$ and different widths d. The plot is normalized to unity at $\vec{r} = 0$, and contour lines for values 1 (*solid line*) and 1/2 (*dotted line*) are drawn in *red*. The image plane is now shifted to $z = 0$ (*vertical green line*)

term of the PSF given in (2). Within the spectral domain $\vec{k}_\perp \cdot \vec{k}_\perp = k_\perp^2 \leq k_0^2$, β_1 yields a real value leading to waves that carry energy to the far field $z \to \infty$. If $k_\perp > k_0$, however, β_1 is purely imaginary so that this part of the wave field contributes exclusively to the near field, $z \gtrsim z_0 - d$. The 3D PSF is then written as $h_3 = h_N + h_F$ where the far-field term,

$$h_F(\vec{R}, z) = \frac{-ik_0}{2\pi} \iint a(\vec{s}) \exp(ik_0 \vec{s}\vec{r})\, d\Omega, \tag{7}$$

is evaluated from (2) within the far-field spectral domain, $0 \leq \theta \leq \pi/2$, being $d\Omega = \sin\theta\, d\theta\, d\phi$ the element of solid angle in spherical coordinates. In (7), the point of observation $\vec{r} = \vec{R} + z\hat{z}$ and the 3D unitary vector $\vec{s} = \vec{s}_\perp + s_z\hat{z}$ is deduced from the dispersion equation $k_0\vec{s} = \vec{k}_\perp + \beta_1\hat{z}$. Finally, the angular spectrum

$$a(\vec{s}) = \frac{i}{\lambda_0} T(\vec{s}) s_z, \tag{8}$$

where $s_z = \cos\theta$. Since $k_\perp = k_0 \sin\theta$, the transmittance T depends exclusively upon the azimuthal coordinate θ, and so does a.

To gain a deep insight into the PSF term h_F, let us consider the limiting case $\delta \to 0$. In this case $T = 1$ and the transverse distribution of the PSF is an Airy disk,

$$h_F(\vec{R}, 0) = \frac{J_1(k_0 R)}{\lambda_0 R}, \tag{9}$$

where J_1 is a Bessel function of the first kind. Along the axis $R = 0$ the PSF may be expressed analytically as

$$h_F(0, z) = \frac{(1 - ik_0 z)\exp(ik_0 z) - 1}{2\pi z^2}. \tag{10}$$

We remark that $|h_F|$ is maximum at the origin, whose central lobe has FWHMs $\Delta_\perp = 0.705\lambda_0$ and $\Delta_z = 1.55\lambda_0$. At $\lambda_0 = 600$ nm we have $\Delta_\perp = 423$ nm and $\Delta_z = 929$ nm. These numbers are roughly in agreement with the numerical simulation performed in Fig. 1(b) at $d = 1.8$ μm revealing that h_F is the dominant part of the PSF. This is also true for higher values of d. Otherwise the near-field component becomes of significance (see subfigure at $d = 600$ nm), even taking the control of the amplitude distribution in the image volume for slabs of a subwavelength width.

We point out that h_F represents a focused wave with focus at the origin $\vec{r} = 0$ and, as a consequence, it may conform to the standard mathematical treatment of apertured spherical beams. In the limiting case $\delta = 0$ it yields an aberration-free focal wave since $a(\vec{s})$ is a real function excepting a constant complex factor [6]; otherwise monochromatic aberrations arise [2]. From (7) we infer that h_F may be written in terms of a 3D Fourier transform of the function $a(\vec{s})$, which has extent in three dimensions and is wrapped around the unit semisphere $\vec{s} \cdot \vec{s} = 1$ and $s_z \geq 0$ [see Fig. 2(a)]. In McCutchen's original paper [4], the function a is coined as the *generalized aperture* describing the patch of solid angle occupied by the Huygenian source at the aperture plane of the converging wave. In our case, however, the transmission is determined by the function T rather than absorption on an opaque screen. Therefore, $a(\vec{s})$ is simply recalled as the generalized ATF of the perfect lens.

The near-field wave h_N might be expressed in the form of (7) if the angular coordinate θ is represented in the complex plane. Setting $\theta = \pi/2 - i\alpha$ and running α from 0 to ∞ allows us to consider the normalized wave vector $\vec{s}$ with real transverse component of modulus $s_\perp = \cosh\alpha > 1$ and purely imaginary axial component $s_z = i\sinh\alpha$. The dispersion equation is conveniently rewritten as $s_\perp^2 - (s_z'')^2 = 1$, where $s_z = s_z' + is_z''$, representing a unit hyperboloid shown in Fig. 2(a). It is immediate that the angular spectrum $a(\vec{s})$ wrapped around such a surface constitutes the second sheet

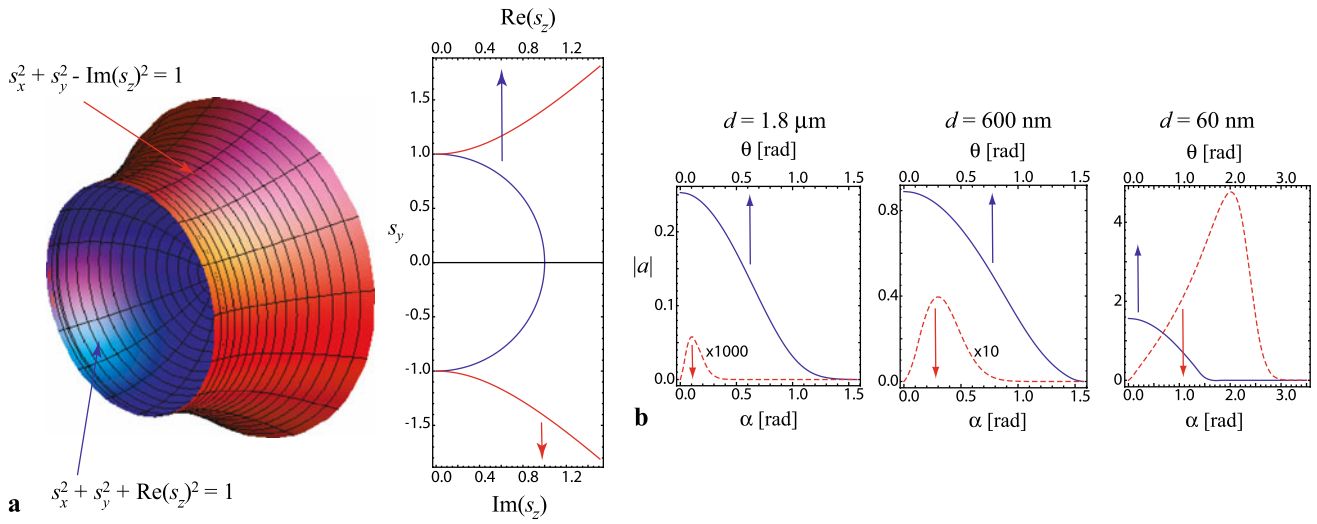

Fig. 2 Spherical and hyperboloidal sheets constituting the generalized ATF are shown in **(a)** in 3D and on the meridional plane $s_x = 0$. In **(b)** we represent the angular spectrum $|a|$ (*in blue*) and the near-field term of the ATF (*in red*) for the numerical simulation of Fig. 1(b)

of the generalized ATF associated with evanescent components of the wave field.

Previously we mentioned that h_3 is singular in a lossless metamaterial lens, caused by the near-field term h_N. In this case, the unbounded function $a(\vec{s})$ modulates the ATF over the hyperboloidal sheet having infinite extent. However, the PSF is bandlimited when $\delta \neq 0$ [7]. As shown in Fig. 2(b), the modulus $|a|$ is maximum at $\theta = 0$ for the far-field term, approaching $\lambda_0^{-1} \exp(-k_0 \delta d)$, and it decreases to zero at $\theta = \pi/2$. Within the near-field regime, $|a|$ grows exponentially at increasing values of α, however attaining a local maximum $|a|_{\max}$ before it decreases for $\alpha \to \infty$. For $d = 60$ nm, the maximum $|a|_{\max} = 4.77\ \mu\mathrm{m}^{-1}$ at $\alpha_{\max} = 2.02$ rad, which corresponds to a normalized spatial frequency $s_\perp = 3.82$ (and $s_z = i3.69$). On the far-field sheet the generalized ATF remains comparatively low since $|a| \leq 1.57\ \mu\mathrm{m}^{-1}$ $[= |a(\theta = 0)|]$. The effective area of the hyperboloidal surface where $a(\vec{s})$ takes significant values also surpasses in several units that from the unit semisphere. On the other hand, for $d = 1.8$ μm, $|a|_{\max} = 5.76 \times 10^{-5}\ \mu\mathrm{m}^{-1}$ at $\alpha_{\max} = 0.104$ rad, associated with a unit vector of $s_\perp = 1.005$ (and $s_z = i0.104$). This is several orders of magnitude lower than the maximum $|a| = 0.253\ \mu\mathrm{m}^{-1}$ given at $\theta = 0$. Expectedly the effective area of $a(\vec{s})$ on the hyperboloid is here a fraction of that from the semisphere.

We conclude that the generalized ATF provides geometrical and analytical arguments in order to derive critically whether h_N represents the dominant contribution to the PSF. This is of relevance since subwavelength resolution is achieved exclusively in such a case.

Superresolving layered lenses made of metamaterials with moderate absorption are limited by a subwavelength width. For microscopy applications, an extended object should be confined in the vicinities of the NRI slab in order to give rise to real images. Moreover, the decay of the wave field from the output plane of the lens leads to inability for producing 3D focusing of energy in spots smaller than λ_0 [3]. However, a quasi-planar object with grooves and small surface defects contains some depth information that might be transmitted through the lens. As illustration we show in Fig. 3 the contour plot of energy density in the image space which is produced by two equienergetic point sources. An incoherent superposition is assumed to get rid of interference phenomena. Both points are separated 120 nm along the transverse direction. We analyze the case that one of these objects O_1 stays closer to the lens than O_2, and therefore its image O_1' remains in a plane (here $z = 0$) further from the lens back face. In this plane the presence of the second image O_2' is imperceptible in virtue of the evanescent nature of its wave field. Moving to the image plane $z = -40$ nm of O_2' it is clearly detected, however, superposed to the strong back tail produced by O_1'. For the lower-absorbing layer ($\delta = 10^{-3}$) the higher superresolving power along the transverse direction is achieved. Nevertheless its back tail at $z < 0$ spreads much faster, hindering the observation of O_2'.

4 Conclusion

In direct analogy with conventional image-forming systems we show that when a NRI planar lens produces an image of a point source the 3D diffraction pattern which results is the 3D Fourier transform of a function that here we called the generalized ATF. This feasible application of the McCutchen analysis [4] relies on the relation between the angular spectrum of the PSF and the lens transmittance in the

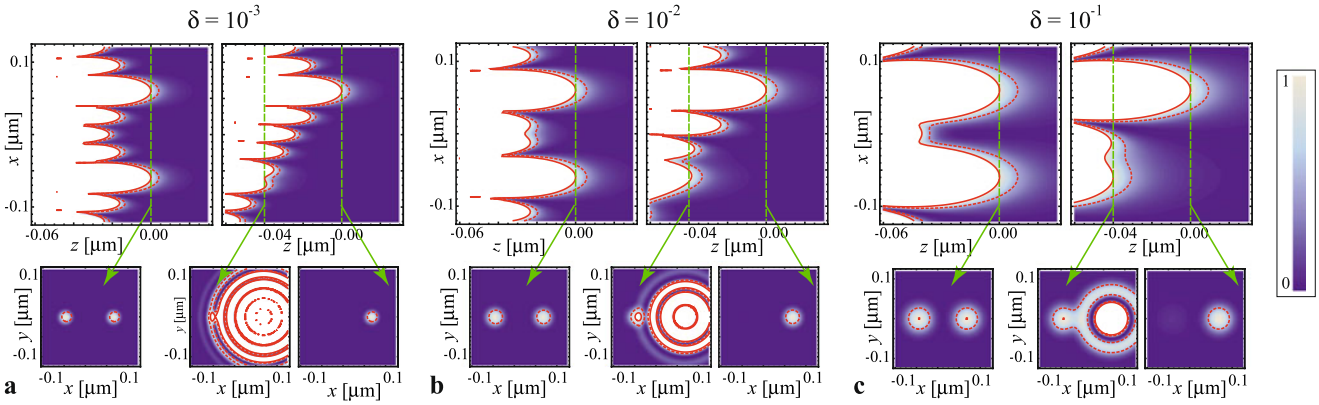

Fig. 3 Energy density in the image volume of two point sources centered at $x = \pm 60$ nm provided under different conditions of absorption and depth

spatial-frequency domain. Particularly, subwavelength resolution is mostly determined by the modulation of the generalized ATF on the hyperboloidal sheet. In connection with this result we have understood that increasing the transverse resolution within the near-field regime may be produced at the cost of loss in depth discrimination.

Acknowledgements This research was funded by Ministerio de Ciencia e Innovación (MICIIN) under the project TEC2009-11635.

References

1. J.B. Pendry, Negative refraction makes a perfect lens. Phys. Rev. Lett. **85**(18), 3966–3969 (2000)
2. M. Nieto-Vesperinas, Problem of image superresolution with a negative-refractive-index slab. J. Opt. Soc. Am. A **21**(4), 491–498 (2004)
3. R. Marques, M.J. Freire, J.D. Baena, Theory of three-dimensional subdiffraction imaging. Appl. Phys. Lett. **89**(21), 211113 (2006)
4. C.W. McCutchen, Generalized aperture and the three-dimensional diffraction image. J. Opt. Soc. Am. **54**(2), 240–242 (1964)
5. P. Yeh, *Optical Waves in Layered Media* (Wiley, New York, 1988)
6. E. Collet, E. Wolf, Symmetry properties of focused fields. Opt. Lett. **5**(6), 264–266 (1980)
7. D.R. Smith, D. Schurig, M. Rosenbluth, S. Schultz, Limitations on subdiffraction imaging with a negative refractive index slab. Appl. Phys. Lett. **82**(10), 1506–1508 (2003)